•工程结构减震与隔震•

DOI:10.12454/j.jsuese.202300931

本刊网刊

极罕遇地震作用下无预紧力变摩擦惯容器消能体系抗震性能分析

赵桂峰[1],刘　伟[2,3],马玉宏[2,3*],孔思华[2,3],陈家川[1],陈兆升[4]

(1.广州大学 土木工程学院,广东 广州 510006;2.广州大学 工程抗震研究中心,广东 广州 510006;
3.广东省地震工程与应用技术重点实验室,工程抗震减震与结构安全教育部重点实验室,广东 广州 510006;
4.青岛市建筑工程管理服务中心,山东 青岛 266071)

摘　要:针对传统摩擦阻尼器在极罕遇或近场脉冲型地震作用下需施加较大预紧力以提供足够的阻尼力,且可能引发耐久性问题这一现状,提出一种无预紧力变摩擦惯容器(NVFI)。首先,对NVFI的组成、工作原理及力学模型进行介绍,指出其通过滚珠丝杠驱动弹簧施加可变正压力,从而在摩擦片之间形成随运动变化的变摩擦阻尼力,呈现出“蝴蝶形”滞回曲线特征。其次,建立NVFI的恢复力计算公式,并以单自由度结构为算例,开展各级地震作用下的非线性动力时程分析,验证NVFI的减震效果和能量耗散能力。研究结果表明:NVFI可在无预紧力条件下实现大吨位的变摩擦阻尼力,有效降低结构位移、速度及加速度响应,且对近场脉冲型地震作用下的减震效果尤为突出。在设防地震水平下,NVFI可分别降低远场、近场脉冲型及非脉冲型地震作用下结构位移响应的46%、56%和34%,同时表现出较好的速度与加速度减震性能。能量分析显示,NVFI可显著降低结构输入的地震能量,改变结构基本频率,使之避开外界地震主频的影响范围。此外,通过分析质量比在0～0.5变化对结构动力响应的影响可知,质量比主要影响结构的速度和加速度响应,对位移响应影响相对较小;NVFI的减震与耗能性能主要依赖其优异的变摩擦阻尼特性,而惯容机制主要是降低地震输入能。

关键词:无预紧力;变摩擦;惯容器;极罕遇地震;抗震性能
中图分类号:TU352.1　　**文献标志码:**A　　**文章编号:**2096-3246(2025)04-0062-09

近年来,汶川、土耳发生地震的震中烈度都远超过其设防烈度,造成极其惨烈的地震灾害。因此,在超烈度极罕遇地震作用下,如何减轻灾害、防止结构倒塌破坏,成为国内外关注的热点[1]。第5代《中国地震动参数区划图》为极罕遇地震作用的分析提供计算依据[2–3]。

极罕遇地震作用下,结构的水平位移可能会显著增加,加剧结构损坏及与相邻结构碰撞的可能性[4];研究表明,结构最大层间位移角超过规范要求时,无法满足正常使用功能阶段的要求[5–6]。虞终军等[7]发现,罕遇、极罕遇地震作用会引起较大的结构残余层间位移角及损伤。吕大刚[8]、王从[9–10]、徐铭阳[11]和Mao[12]等发现巨震下的倒塌概率为54.7%,说明巨震下结构倒塌概率比常规地震更大。而采取合适的减隔震控制措施将成为应对极罕遇地震作用的有效手段,包括采用惯容与黏滞阻尼装置降低结构响应[13–15],以及利用多级屈服与损伤控制阻尼器提升结构韧性[16–18]。

建筑消能减震技术规程[19]要求阻尼器在小震、中震和大震都具备良好的变形能力和消耗地震能量的能力,其极限位移应大于消能器设计位移的120%,速度相关型阻尼器极限速度应大于设计速度的120%。在极罕遇地震作用下,阻尼器需满足更高的性能指标,提供更大的阻尼力、设计位移的冗余度,才能确保其在极罕遇地震作用下性能不失效或不发生破坏。因此,越来越多的学者在此方面开展深入研究。秦凯等[20]提出一种可使耗能能力放大的黏滞消能伸臂装置,在罕遇地震作用下能有效地控制主体结构的层间位移角、基底剪力等地震响应和塑性损伤,综合提高阻尼伸臂系统的能量耗散效率;Huang等[4]研究表明,

收稿日期:2023－11－19　**修回日期:**2024－05－13　**网络出版日期:**2024－05－14
基金项目:国家重点研发计划项目(2022YFC3801201;2019YFE0112500);国家自然科学基金项目(52378499;52308488;52078150);广东省基金面上项目(2023A1515010072)
作者简介:赵桂峰(1972—),男,副教授. 研究方向:结构减隔震控制. E-mail:zgfzth@gzhu.edu.cn
* **通信作者:**马玉宏,研究员,E-mail:myhzth@gzhu.edu.cn

在极罕遇地震作用下，质量调谐阻尼器需串联或并联基础隔震，才会有较好的减震效果；Miyamoto 等[21]考虑极罕遇地震，进行全面地分析和实验研究，评估黏滞阻尼器结构在极罕遇地震下的倒塌性能；Wu 等[22]考虑强震，对建筑-阻尼器系统的抗震性能及阻尼器失效的影响进行了系统评价，包括屈曲约束支撑（BRB）、摩擦阻尼器（FD）、黏滞阻尼器（VD）和黏弹性阻尼器（VED），结果表明，在强震作用下，建筑-阻尼器系统响应较大，存在阻尼器失效的可能。

传统摩擦阻尼器通过预紧力螺栓施加预紧力[23–25]提供滑动摩擦力，若起滑力较大，阻尼器在小、中震中可能无法发挥耗能作用；若起滑力较小，则在大震、极罕遇地震中无法提供充分的耗能能力，进而难以取得预期的减震效果，且阻尼器位移容易超过其极限能力[26–27]。此外，长期处于较大预紧力作用下的摩擦材料之间，易出现冷黏结、冷凝固和预紧力易松弛等问题，导致其力学性能难以准确预测[28]。陈家川等[29]提出一种无预紧力变摩擦惯容器，给出其力学简化模型，并通过拟静力试验验证其作用机理和力学模型的正确性；推导了简谐荷载作用下 NVFI 单自由度减震体系的位移解析解和动力放大系数，并进行相关参数分析。研究表明：该消能装置无须施加预紧力，可随位移变化提供变摩擦力，可自适应调节阻尼力大小，克服了传统摩擦阻尼器存在的问题，具备较强的耗能能力。为促进其在实际工程中应用，有必要进一步探究 NVFI 减震体系的减震控制效果。

本文在简单介绍 NVFI 工作机理和力学模型的基础上，对 NVFI 减震体系的减震控制效果、滞回特性及累积耗能进行分析，同时探究质量比变化对控制效果的影响，进而揭示 NVFI 应对极罕遇近断层脉冲型地震作用的有效性，为其工程应用提供依据。

1　NVFI 的力学模型

NVFI 是利用弹簧的压缩变形在摩擦片与圆环形钢板之间提供正压力来产生摩擦力。地震作用下，滚珠丝杠驱动弹簧，其对摩擦片施加的正压力不断变化，从而使摩擦力也相应变化。同时，基于滚珠丝杠机构的位移和阻尼力放大效应来消耗地震能量，NVFI 示意图如图 1 所示。

根据陈家川等[29]研究，NVFI 提供的阻尼力为：

$$F_{\mathrm{NVFI}}=F_{\mathrm{d}}\,\mathrm{sgn}(\dot{x})+m_{\mathrm{d}}\ddot{x}+k_{\mathrm{d}}x \tag{1}$$

$$F_{\mathrm{d}}=\mu\alpha_{\mathrm{n}}k_{\mathrm{d}}|x|=\frac{4}{3}\pi\mu\frac{1}{\eta L_{\mathrm{d}}}\cdot\frac{r_1^2+r_1r_2+r_2^2}{r_1+r_2}k_{\mathrm{d}}|x| \tag{2}$$

$$m_{\mathrm{d}}=\frac{2\pi^2(r_1^2+r_2^2)}{\eta L_{\mathrm{d}}^2}m_0 \tag{3}$$

式（1）～（3）中：F_{NVFI} 为 NVFI 阻尼力；F_{d} 为随位移变化的放大摩擦力；m_{d} 为放大后质量；F_{d}、m_{d} 均与构造参数有关；x、$\dot{x}$ 和 $\ddot{x}$ 分别为位移、速度和水平加速度；μ 为摩擦系数；r_1 和 r_2 分别为圆环形钢板的内半径和外半径；η 为滚珠丝杠传动效率；k_{d} 为弹簧刚度；m_0 为圆环形钢板质量；L_{d} 为滚珠丝杠的导程；$\mathrm{sgn}(\dot{x})$ 为关于滚珠丝杠速度的符号函数，当 $\dot{x}\le 0$ 时，$\mathrm{sgn}(\dot{x})=-1$，当 $\dot{x}>0$ 时，$\mathrm{sgn}(\dot{x})=1$，当 $\dot{x}=0$ 时，丝杠处于静止状态。

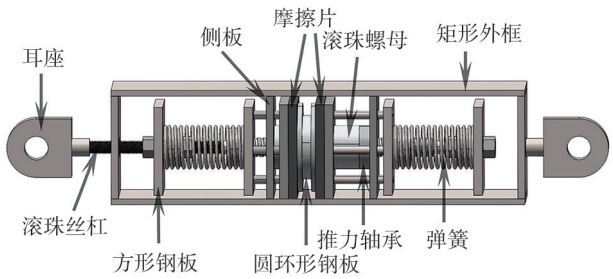

图 1　NVFI 示意图

Fig. 1　NVFI diagram

NVFI 简化力学模型如图 2 所示。NVFI 的滞回模型如图 3 所示，由具有“蝴蝶形”滞回曲线的放大摩擦力 $F_{\mathrm{d}}\,\mathrm{sgn}(\dot{x})$、正刚度效应的弹簧弹性力 $k_{\mathrm{d}}x$ 及负刚度效应的放大惯性力 $m_{\mathrm{d}}\ddot{x}$ 这 3 部分叠加而成。

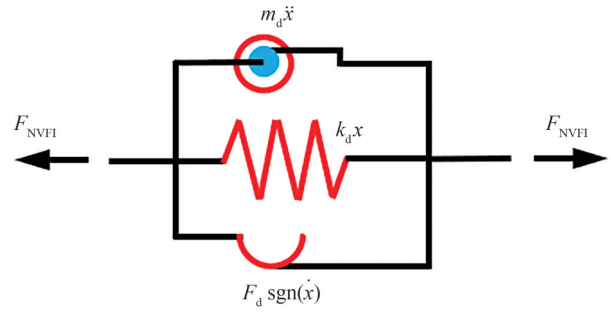

图 2　NVFI 简化力学模型

Fig. 2　Simplified mechanical model of NVFI

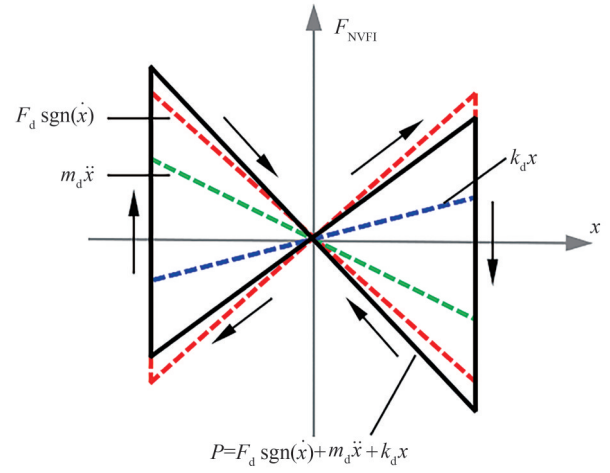

图 3　NVFI 的滞回模型

Fig. 3　Hysteretic model of NVFI

2 NVFI单自由度减震体系的计算模型及地震波选取

2.1 计算模型

陈家川等[29]在研究中，通过拟静力试验验证了所提出的NVFI力学模型。试验结果表明，该模型能够较好地描述NVFI装置在不同加载条件下的力−位移关系和耗能特性，为本文的理论分析奠定了基础[29]。为进一步验证NVFI力学模型在动力分析中的适用性，并提高计算效率，本文选取单自由度结构（SDOF）作为分析对象。NVFI单自由度减震体系（SDOF-NVFI）计算模型如图4所示，其在地震作用下的运动方程为：

$$\begin{cases} m\ddot{x}+c\dot{x}+kx+F_{\mathrm{NVFI}}=-m\ddot{x}_{\mathrm{g}}, \\ F_{\mathrm{NVFI}}=F_{\mathrm{d}}\,\mathrm{sgn}(\dot{x})+m_{\mathrm{d}}\ddot{x}+k_{\mathrm{d}}x \end{cases} \tag{4}$$

式中，m为单自由度体系的质量，c为阻尼系数，k为单自由度体系的刚度，$\ddot{x}_{\mathrm{g}}$为地震输入加速度。

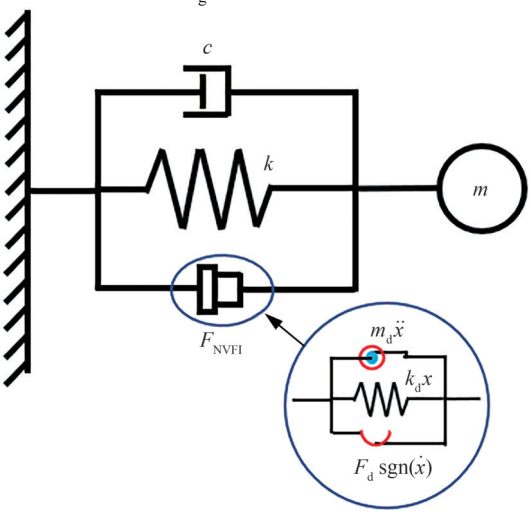

图4 NVFI单自由度减震体系的计算模型

Fig. 4 Calculation model of NVFI single-degree-of-freedom damping system

2.2 地震波选取

为研究在不同场地地震波作用下NVFI减震耗能的有效性，选取FEMA P695中推荐的近断层脉冲、近断层非脉冲及远场地震动3组（每组各7条），地震记录参数如表1所示。表1中，P_{GA}为地面加速度峰值，P_{GV}为地面速度峰值。分析过程中对地震波进行归一化处理，具体分析时可采用调幅的方法调整设防地震、罕遇地震和极罕遇地震对应的加速度峰值，各组地震波平均加速度反应谱如图5所示。由图5可知：在0～0.5 s内，3种类型地震动平均加速度反应谱值相近，在0.5～4.0 s内的大部分周期对应的平均加速度反应谱值大小关系为：近断层脉冲型地震大于远场地震动，远场地震动大于近断层非脉冲型地震动。

表1 地震记录参数

Tab. 1 Ground motion records parameters

地震波类型	地震波编号	地震波名称	P_{GA}	$P_{\mathrm{GV}}\cdot P_{\mathrm{GA}}^{-1}$
近断层脉冲	181	Imperial Valley−06	0.44g	0.26
	802	Loma Prieta	9.40g	0.15
	821	Erzican（Turkey）	0.49g	0.20
	879	Landers	0.79g	0.18
	1063	Northridge−01	0.87g	0.20
	1086	Northridge−01	0.73g	0.17
	1165	Kocaeli（Turkey）	0.22g	0.14
近断层非脉冲	126	Gazli（USSR）	0.71g	0.10
	160	Imperial Valley−06	0.76g	0.06
	165	Imperial Valley−06	0.28g	0.11
	495	Nahanni（Canada）	1.18g	0.04
	753	Loma Prieta	0.51g	0.09
	825	Cape Mendocino	1.43g	0.09
	1004	Northridge−01	0.73g	0.10
远场	68	San Fernando	0.21g	0.09
	125	Friuli（Italy）	0.35g	0.09
	721	Superstition Hills	0.36g	0.13
	725	Superstition Hills	0.45g	0.08
	953	Northridge	0.52g	0.12
	1158	Kocaeli（Turkey）	0.36g	0.17
	1787	Hector Mine	0.34g	0.13

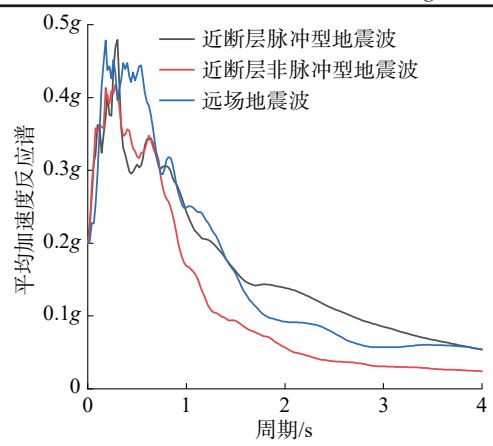

图5 各组地震波平均加速度反应谱

Fig. 5 Average acceleration response spectrum of each group of ground motion records

3 NVFI单自由度减震体系的减震效果分析

取单层框架结构的质量、刚度和阻尼比分别为50 660 kg、2 000 kN/m和5%[30]，结构非线性模型采用Bouc−Wen模型，屈服后刚度比0.1，屈服位移12 mm。NVFI摩擦系数0.2，圆环形钢板内径和外径分别为0.1和0.2 m，圆环形刚板质量5 kg，丝杠导程0.02 m，弹簧刚度为15 kN/m。

3.1 减震控制效果分析

通过计算分析可知，3组地震波在设防地震（0.2g）、罕遇地震（0.4g）和极罕遇地震（0.6g）作用下，NVFI减震体系的最大位移、速度及加速度的结构最大反应平均减震率如图6所示。

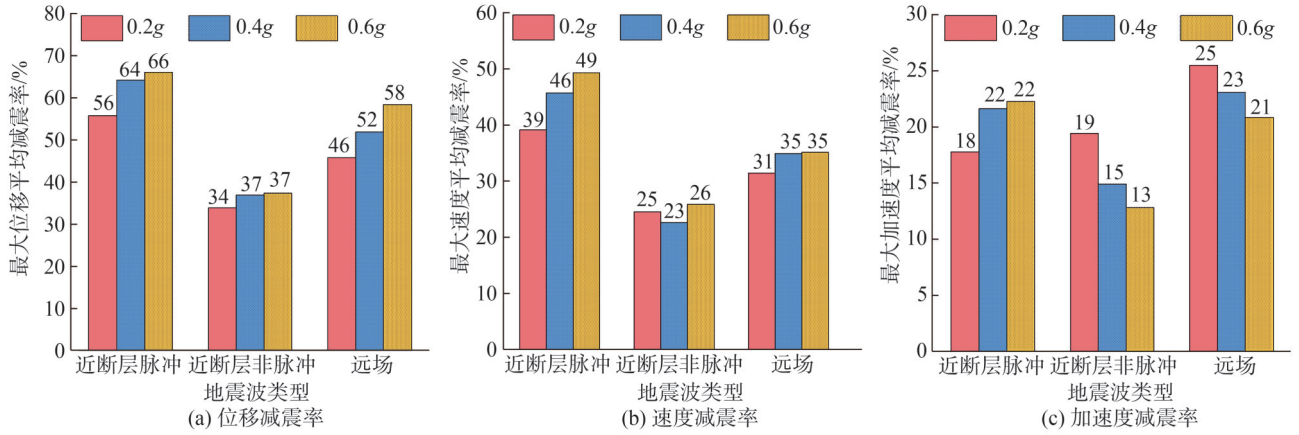

图6　结构最大反应平均减震率

Fig. 6　Average damping ratio of structural maximum res-ponse

由图6可知：1）在相同地震动加速度峰值输入时，对于3组地震波整体而言，最大位移平均减震效果优于最大速度和最大加速度平均减震效果；2）脉冲型和远场地震波的减震效果要明显优于近断层非脉冲型地震，因为单自由度结构模型的周期为1 s，此处所选脉冲型地震动和远场地震动的平均反应谱值要大于非脉冲地震波，同时，脉冲型地震动有脉冲效应，导致脉冲型地震下的结构位移大于非脉冲下的位移，由于NVFI具有变摩擦特性，位移越大，NVFI出力越大，对脉冲型和远场地震波控制效果比非脉冲型好；3）随着输入地震加速度峰值的增大，近断层脉冲型地震动的最大位移、速度和加速度平均减震率均呈增大趋势，极罕遇地震下减震效果尤为明显；而对于近断层非脉冲地震动和远场地震动，最大位移平均减震率呈增大趋势，最大速度平均减震率变化不明显，最大加速度减震率呈下降趋势，表明NVFI对极罕遇脉冲型地震取得了优异的减震控制效果。

3.2　地震反应时程分析

在极罕遇脉冲型Erzican、近断层非脉冲Imperial Valley−06、远场Kocaeli地震波作用下（0.6*g*），有控和无控结构的位移、速度和加速度的时程曲线如图7所示。

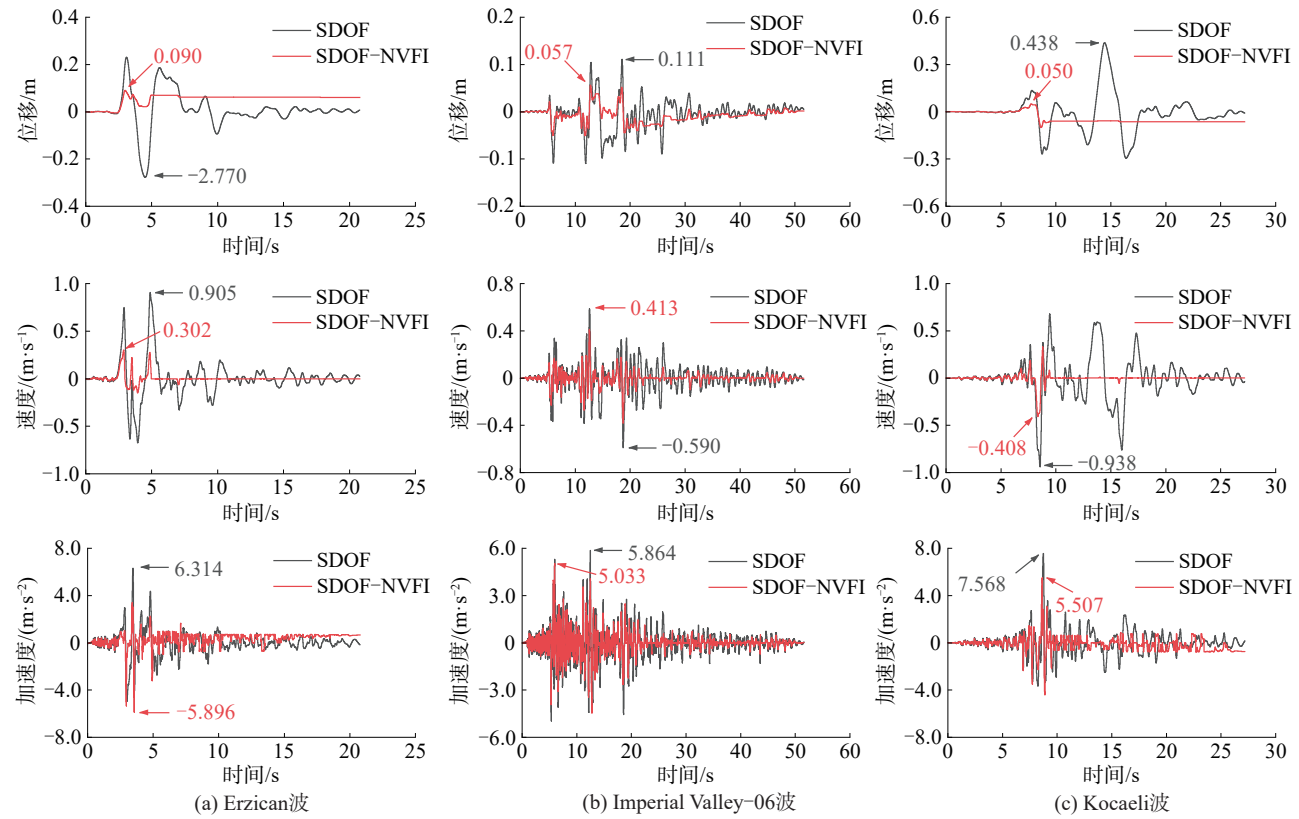

图7　3组地震波极罕遇地震作用下的结构反应时程曲线（0.6*g*）

Fig. 7　Time-history curves of structural response under three seismic waves (0.6*g*)

由图 7 可见：在 3 组极罕遇地震下，NVFI 对位移、速度和加速度的整体减震效果均较好，位移、速度整体控制效果优于加速度；近断层脉冲型地震动和远场地震动的整体减震效果优于非脉冲型地震动，且随着输入地震加速度峰值的增加，位移、速度和加速度整体控制效果有所提高。

3.3 NVFI 滞回特性分析

3 组地震波作用下 NVFI 滞回曲线如图 8 所示。由图 8 可知，NVFI 呈现出明显的位移相关性变摩擦效应，滞回曲线与第 3.1 节理论力学模型吻合。

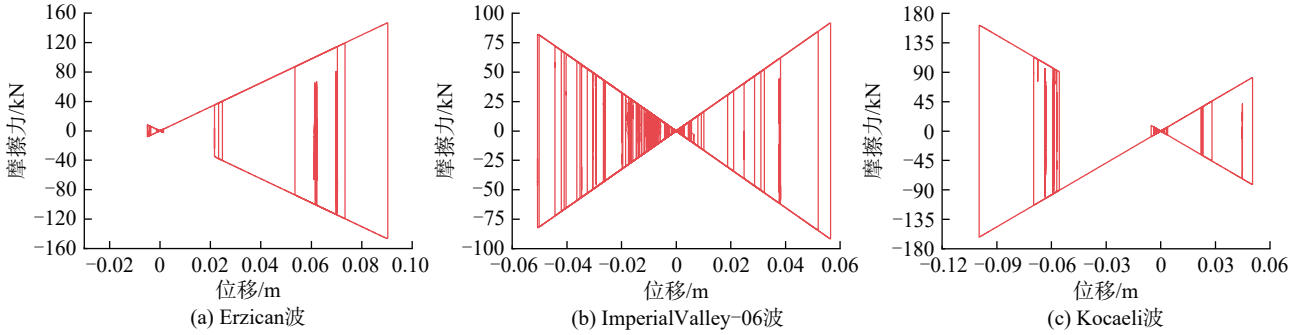

图 8 3 组地震波作用下 NVFI 滞回曲线（0.6*g*）

Fig. 8 Hysteretic curves of NVFI under three seismic waves (0.6*g*)

3.4 耗能能力分析

无控结构和 NVFI 减震体系累积耗能时程曲线分别如图 9 和 10 所示。由图 9 和 10 可知：无控结构中，地震波输入能量主要依赖结构变形和阻尼耗能；有控结构中，地震总输入能量相对于无控结构会减小。这是由于 NVFI 放大质量改变了结构自振周期。同时，地震输入能主要由 NVFI 耗散，结构变形能与无控结构相比大幅减小，结构层间位移也大幅降低。在极罕遇地震下，地震总输入能与 NVFI 耗能曲线之间的距离最小，表明 NVFI 取得了最佳的耗能减震效果。

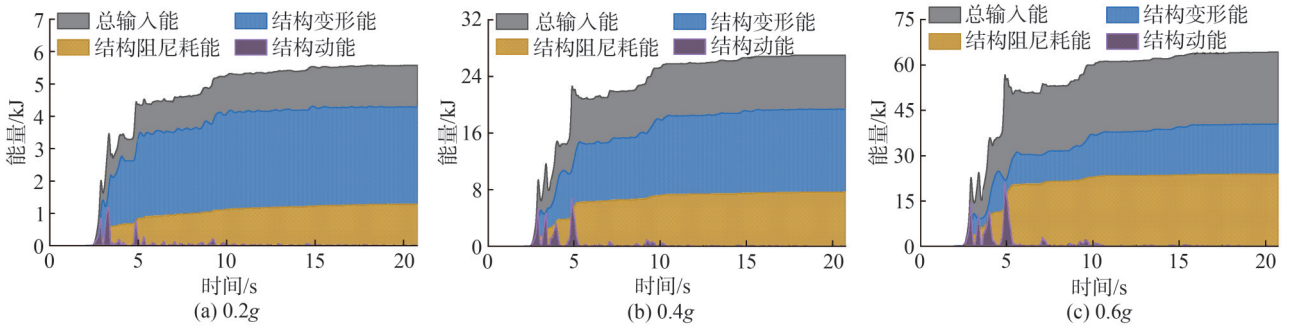

图 9 无控结构累积耗能时程曲线

Fig. 9 Cumulative energy dissipation time-history curves of uncontrolled structure

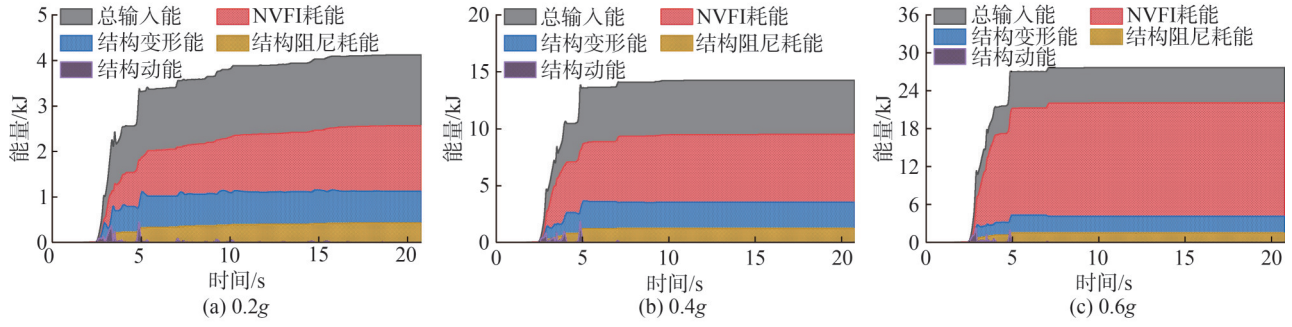

图 10 NVFI 减震体系累积耗能时程曲线

Fig. 10 Cumulative energy dissipation time-history curves of NVFI damping system

3 组地震波在不同加速度峰值作用下，NVFI 平均耗能率（NVFI 耗能与总输入能之比）如图 11 所示。由图 11 可知：对于 3 组不同类型地震波，NVFI 均取得了 50% 以上的耗能效果。同一类地震波，随着输入加速度峰值增大，NVFI 平均耗能率呈现上升的趋势，对于极罕遇脉冲型地震动更为明显。说明 NVFI 能较好地耗散极罕遇及近断层脉冲型地震动的输入能量，体现了稳定可靠的减震性能。

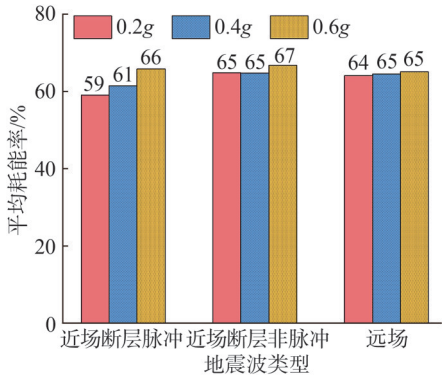

图 11　NVFI 平均耗能率

Fig. 11　Average energy dissipation rate of NVFI

4　NVFI 与惯容器减震效果对比分析

当 NVFI 的弹簧刚度为 0 时，则 NVFI 的阻尼力等于其放大惯性力，此时 NVFI 相当于一个惯容器（Inerter）。对无控结构、Inerter 减震体系和 NVFI 减震体系反应进行对比分析，探索 Inerter 质量变化对最大减震率、整体减震效果的影响，并与 NVFI 减震效果进行对比。设 NVFI 的弹簧刚度为 100 kN/m，取质量比（$\beta=m_d/m$）变化区间为 0～0.5。

4.1　减震效果对比

近断层和远场地震作用下质量比变化对减震效果的影响规律分别如图 12 和 13 所示。由图 12 和 13 可知：在不同地震类型作用下，两种减震体系中，随质量比增大，位移、速度和加速度峰值减震率大都明显增大；相比 Inerter，NVFI 的减震控制效果更为明显，且随质量比增大 NVFI 的位移减震效果增加不明显，表明其主要依靠变摩擦阻尼耗能。

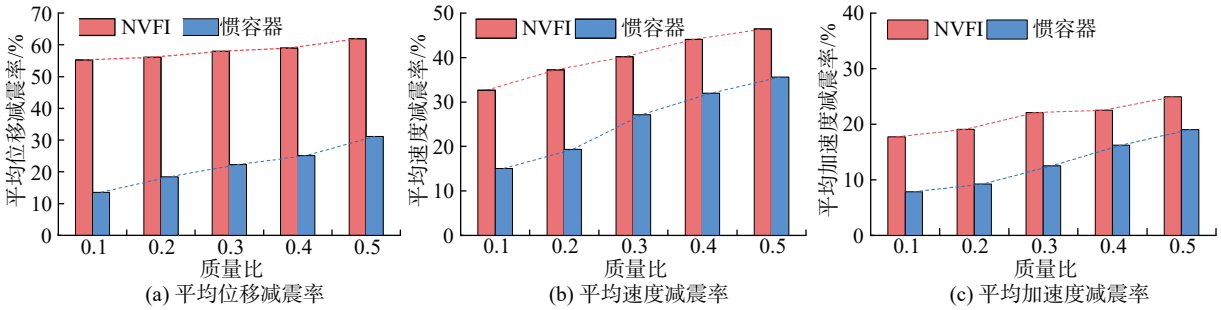

图 12　近断层地震作用下质量比变化对减震效果的影响规律

Fig. 12　Influence of mass ratio on damping effect under near-field earthquake

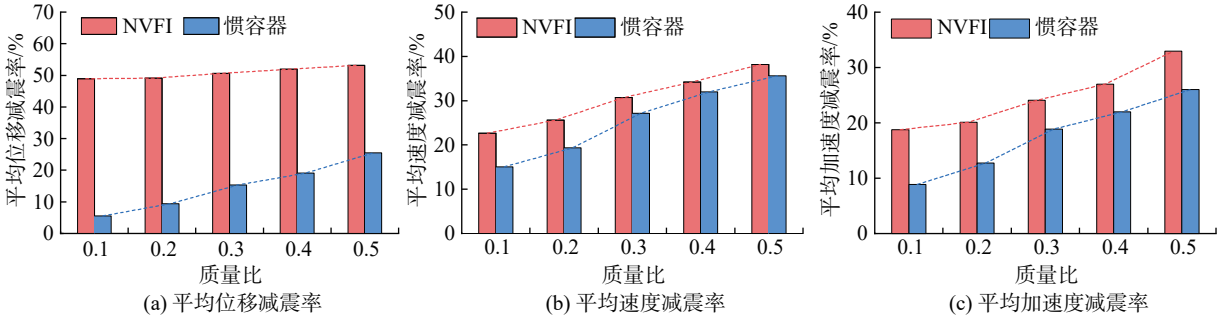

图 13　远场地震作用下质量比变化对减震效果的影响规律

Fig. 13　Influence of mass ratio on damping effect under far-field earthquake

4.2　累积耗能对比

远场 Kocaeli 波作用下质量比分别为 0.1、0.5 时，Inerter 减震体系和 NVFI 减震体系的累积耗能时程曲线分别如图 14 和 15 所示。

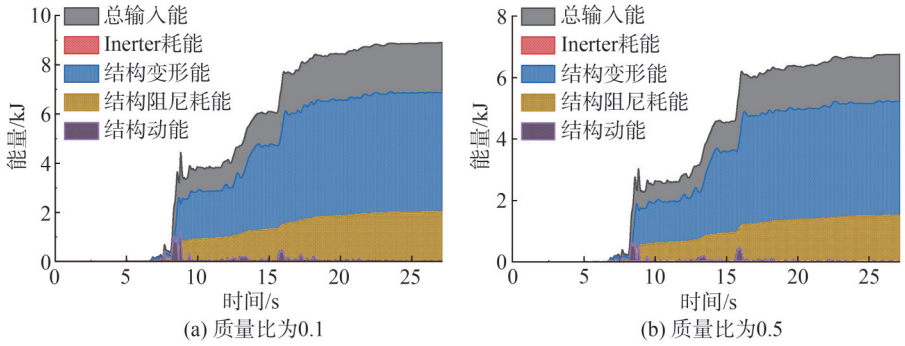

图 14　Inerter 减震体系的累积耗能时程曲线

Fig. 14　Cumulative energy dissipation time-history curves of Inerter damping system

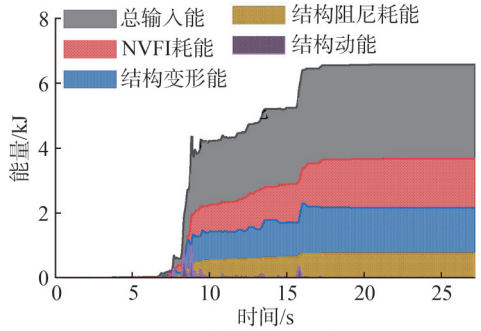

(a) 质量比为0.1

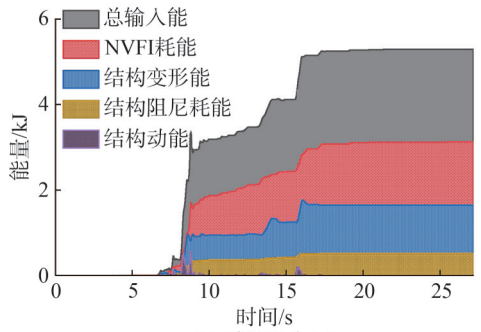

(b) 质量比为0.5

图15 NVFI减震体系的累积耗能时程曲线

Fig. 15 Cumulative energy dissipation time-history curves of NVFI damping system

由图14和15可知：惯容器基本不耗散地震输入能量，但随质量比增大，惯容器和NVFI的放大质量在一定程度上延长了结构自振周期，使减震体系的总输入能有所减小；Inerter减震体系中，地震输入能主要由结构变形耗散；NVFI减震体系中，地震输入能主要由NVFI和结构变形耗散，进一步验证了NVFI中变摩擦机制的必要性及耗能有效性。

5 结 论

本文在前期对简谐荷载作用下NVFI单自由度减震体系的位移解析解和动力放大系数的研究基础上，简介了NVFI的工作机理和力学模型，对NVFI单自由度减震体系进行了减震控制效果分析，并研究了质量比变化对减震效果的影响。主要结论如下。

1）地震作用下，NVFI无须施加预紧力就可提供变阻尼力，具有摩擦力、位移和惯性质量放大效应，呈现出“蝴蝶形”滞回特征，克服了传统摩擦阻尼器的不足，可自适应极罕遇地震和近断层脉冲型地震对大吨位阻尼器的减震需求。

2）在近断层脉冲、非脉冲及远场地震作用下，对设防、罕遇、极罕遇地震，NVFI减震体系的位移、速度、加速度均可取得较好的减震控制效果，体现了稳定可靠的减震性能，尤其对极罕遇脉冲型地震可取得更佳的减震控制效果，具有较好的工程应用前景。

3）质量比变化区间为0～0.5时，单纯惯容器基本不耗散地震输入能量，但随质量比增大，惯容器和NVFI的放大质量在一定程度上延长了结构自振周期，使减震体系的总输入能有所减小；NVFI减震体系中，地震输入能主要由NVFI和结构变形耗散，进一步验证了NVFI中变摩擦机制的必要性及耗能有效性。

参考文献：

[1] Tan Qian,Wu Wei,Zhang Yaoting.Seismic performance analysis of multi-layer RC frame structures under extre-mely rare earthquakes[J].Earthquake Engineering and Engineering Dynamics,2019,39(4):170–177.[谭倩,吴谓,张耀庭.极罕遇地震作用下多层RC框架结构抗震性能分析[J].地震工程与工程振动,2019,39(4):170–177.]

[2] 国家质量监督检验检疫总局,中国国家标准化管理委员会.中国地震动参数区划图:GB 18306—2015[S].北京:中国标准出版社,2016.

[3] Li Qiaoping,Zhao Min.The 4th anniversary of the implementation of China earthquake motion parameter zoning map [J].Overview of Disaster Prevention,2020(3):19–21.[李巧萍,赵敏.《中国地震动参数区划图》施行4周年[J].防灾博览,2020(3):19–21.]

[4] Huang Xiao,Hu Zhixiang,Liu Yunlin,et al.Study on seismic performance of TID–LRB hybrid control system under multi-level earthquakes[J].Buildings,2022,12(9):1465.

[5] Qi Qiming,Shao Changjiang,Huang Hui,et al.Transverse seismic mitigation of railway continuous girder bridge with double-column ultra-high piers based on BRBs[J].Journal of Vibration and Shock,2022,41(7):182–192.[漆启明,邵长江,黄辉,等.基于BRB的铁路双柱式超高墩连续梁桥横向减震研究[J].振动与冲击,2022,41(7):182–192.]

[6] Wang Yuxiang,Ye Kun.Seismic performance analysis of LRB base-isolated multi-story structures subjected to multi-level earthquakes[J].Journal of Building Structures,2023,44(11):1–14.[王昱翔,叶昆.多级地震作用下LRB隔震多层结构抗震性能分析[J].建筑结构学报,2023,44(11):1–14.]

[7] Yu Zhongjun,Li Xin,Wang Jianfeng,et al.Seismic resilience design of a super high-rise office building[J].Journal of Building Structures,2022,43(8):45–55.[虞终军,李歆,王建峰,等.某超高层办公楼结构抗震可恢复性能设计[J].建筑结构学报,2022,43(8):45–55.]

[8] Lv Dagang,Zhou Zhou,Wang Cong,et al.Uniform risk-targeted definitions and decision-making of four seismic design levels considering very rare earthquake[J].China Civil Engineering Journal,2018,51(11):41–52.[吕大刚,周洲,王丛,等.考虑巨震的四级地震设防水平一致风险导向定义与决策分析[J].土木工程学报,2018,51(11):41–52.]

[9] Wang Cong,Lv Dagang.Parameter decision and parameter influence analysis of risk-oriented ground motion[J].Journal of Building Structures,2020,41(Supp2):44–52.[王丛,吕大刚.风险导向地震动参数决策及参数影响分析[J].建筑结构学报,2020,41(增刊2):44–52.]

[10] Wang Cong,Lu Dagang.Analysis of risk-targeted decision parameters of seismic ground motions based on seismic design code and ground motion zonation map of China[J].

Journal of Building Structures,2020,41(8):19–28.[王丛,吕大刚.基于抗震规范和地震动区划图的风险导向地震动决策参数分析[J].建筑结构学报,2020,41(8):19–28.]
[11] Xu Mingyang, Wang Cong, Dong Yao, et al. Study on uniform collapse risk design methods for building structures under very rare earthquakes[J]. Journal of Building Structures,2022,43(7):253–263.[徐铭阳,王丛,董尧,等.极罕遇地震作用下建筑结构一致风险抗倒塌设计方法研究[J].建筑结构学报,2022,43(7):253–263.]
[12] Mao Chenxi, Wang Zhenying. Seismic performance evaluation of a self-centering precast reinforced concrete frame structure[J]. Earthquake Engineering and Engineering Vibration,2021,20(4):943–968.
[13] Ji Xiaodong, Jia Ruofan, Wang Lijun, et al. Seismic design and performance assessment of a retrofitted building with tuned viscous mass dampers(TVMD)[J]. Engineering Structures, 2024,305:117688.
[14] Huang Xiao, Hu Zhixiang, Liu Yunlin, et al. Study on seismic performance of TID−LRB hybrid control system under multi-level earthquakes[J]. Buildings,2022,12(9):1465
[15] Zhang Guanping, Liu Yanhui, Tan Ping, et al. Study on optimization of passive viscous damper and passive hybrid control seismic response[J]. Advanced Engineering Sciences,2020,52(3):70–77.[张冠平,刘彦辉,谭平,等.基于主动控制优化被动黏滞阻尼器及混合隔震研究[J].工程科学与技术,2020,52(3):70–77.]
[16] Lin Xuchuan, Chen Yian, Yan Jiabao, et al. Seismic behavior of welded beam-to-column joints of high-strength steel-moment frame with replaceable damage-control fuses[J]. Journal of Structural Engineering,2020,146(8):04020143.
[17] Zhai Zhipeng, Liu Yanhui, Guo Wei, et al. A seismic resilient design method for structures equipped with two-level yielding dampers, accounting for extremely rare earthquakes[J]. Engineering Structures,2023,294:116797.
[18] Pu Rui, Li Qianqian, Wang Jianze, et al. Performance study of rotational-based metallic damper and engineering application in a complex power plant structure[J]. Advanced Engineering Sciences,2024,56(2):162–171.[蒲瑞,李倩倩,王健泽,等.转角位移型阻尼器性能研究及工程应用[J].工程科学与技术,2024,56(2):162–171.]
[19] 中华人民共和国住房和城乡建设部.建筑消能减震技术规程:JGJ 297—2013[S].北京:中国建筑工业出版社,2013.
[20] Qin Kai, Ge Dongdong, Li Pei, et al. Research on seismic reduction effect of super high-rise structure with amplified viscous energy dissipation extension arm[J]. Journal of Building Structures,2022,43(Supp1):196–204.[秦凯,閤东东,李培,等.超高层建筑结构放大型黏滞消能伸臂减震效果研究[J].建筑结构学报,2022,43(增刊1):196–204.]
[21] Miyamoto H K, Gilani A S J, Wada A, et al. Limit states and failure mechanisms of viscous dampers and the implications for large earthquakes[J]. Earthquake Engineering & Structural Dynamics,2010,39(11):1279–1297.
[22] Wu Xiaoli, Guo Wei, Hu Ping, et al. Seismic performance evaluation of building-damper system under near-fault earthquake[J]. Shock and Vibration,2020,2020:2763709.
[23] Shi Wenlong, Zhang Haobo. Research progress of friction dampers[J]. China Earthquake Engineering Journal, 2022, 44(1):1–16.[石文龙,张浩波.摩擦阻尼器的研究进展[J].地震工程学报,2022,44(1):1–16.]
[24] Zhang Yumin, Gu Yuzhen. Research on the application of friction damper in building structure vibration reduction[J]. Building Structure,2018,48(Supp2):387−392.[张玉敏,谷玉珍.摩擦阻尼器在建筑结构减震应用的现状研究[J].建筑结构,2018,48(增刊2):387–392.]
[25] Liu Yunshuai, Han Jianping, Wang Xiaoqin. Investigation on seismic performance of bridge with self-centering friction dampers[J]. Advanced Engineering Sciences,2018,50(6):77–83.[刘云帅,韩建平,王晓琴.具自复位摩擦阻尼器的桥梁隔震性能研究[J].工程科学与技术,2018,50(6):77–83.]
[26] Jaisee S, Yue Feng, Ooi Y H. A state-of-the-art review on passive friction dampers and their applications[J]. Engineering Structures,2021,235:112022.
[27] Gagnon L, Morandini M, Ghiringhelli G L. A review of friction damping modeling and testing[J]. Archive of Applied Mechanics,2020,90(1):107–126.
[28] Christopoulos C, Filiatrault A. Principles of passive supplemental damping and seismic isolation[M]. Pavia:IUSS Press,2006.
[29] Chen Jiachuan, Zhao Guifeng, Ma Yuhong, et al. Development of non-preload variable friction damper and dynamic characteristics analysis under harmonic excitation[J]. Earthquake Engineering and Engineering Dynamics,2023,43(2):212–221.[陈家川,赵桂峰,马玉宏,等.无预紧力变摩擦阻尼器的研发与简谐激励下的动力特性分析[J].地震工程与工程振动,2023,43(2):212–221.]
[30] Hatzigeorgiou G D, Pnevmatikos N G. Maximum damping forces for structures with viscous dampers under near-source earthquakes[J]. Engineering Structures,2014,68:1–13.

Seismic Performance Analysis of Energy Dissipation Building with Non-preload Variable Friction Inerter Under Extremely Rare Earthquake

ZHAO Guifeng[1], *LIU Wei*[2,3], *MA Yuhong*[2,3*], *KONG Sihua*[2,3], *CHEN Jiachuan*[1], *CHEN Zhaosheng*[4]

(1.School of Civil Engneering, Guangzhou University, Guangzhou 510006, China;
2.Earthquake Engneering Research & Test Center, Guangzhou University, Guangzhou 510006, China;
3.Guangdong Provincial Key Laboratory of Earthquake Engneering and Applied Technology, Key Laboratory of Earthquake Resistance, Earthquake Mitigation and Structural Safety, Ministry of Education, Guangzhou 510006, China;
4.Qingdao Construction Engneering Management Service Center, Qingdao 266071, China)

Abstract:

Objective Traditional energy dissipation technologies provide an effective solution to mitigate the seismic responses of buildings. There are two types of energy dissipation devices based on their operational characteristics: velocity-dependent dampers and displacement-dependent dampers.

Friction dampers (FDs), as a category of displacement-dependent energy dissipation devices, exhibit several common advantages, such as good energy dissipation capacity, satisfactory mechanical performance, and ease of fabrication and installation. Therefore, they have received extensive attention from researchers in recent years. Buildings can require large damping forces under extremely rare or near-fault earthquake events, which necessitate that existing FDs apply a high preload to deliver sufficient reaction forces. However, introducing an excessive preload force can be impractical and uneconomical for current FDs. For example, the damping force of existing FDs can need to reach 1 000 kN for buildings subjected to a severe or near-fault earthquake event, resulting in a required preload force of 10 000 kN when the friction coefficient is assumed to be 0.1. In addition, FDs with a specified preload force still face durability issues such as cold bonding, cold solidification, and preload relaxation. Therefore, this study aims to develop a non-preload variable friction inerter (NVFI), which provides satisfactory damping force and significant energy dissipation without relying on preload force.

Methods The proposed NVFI mainly consisted of a ball screw, rotational plate, friction plate, spring, and two thrust bearings. One terminal of the ball screw was fixed to the structure using an ear plate. The ball screw of the NVFI generated axial motion when the structure reciprocally shook under seismic earthquakes, and the springs were driven to reciprocal motion, resulting in a variable positive pressure of the friction plate. Therefore, the butterfly-shaped hysteretic behavior of the proposed NVFI was found based on the friction mechanism mentioned above. Then, the restoring force formula of the proposed NVFI was further established. Then, seismic performance mitigation of a single-degree-of-freedom (SDOF) system under different hazard levels was conducted to evaluate the effectiveness and advantages of the proposed NVFI quantitatively. A 5% damping SDOF system with a mass of 50 660 kg and elastic stiffness of 2 000 kN/m was adopted as the analytical model. A Bouc−Wen elasto-plastic model was employed in the SDOF system with a yield strength of 24 kN and post-elastic stiffness of 200 kN/m. The SDOF system with and without the proposed NVFI was considered and denoted as SDOF–NVFI and SDOF, respectively. Three groups of different ground motion records, including far-field, near-fault pulse, and near-fault non-pulse ground motion records, were selected to perform the nonlinear dynamic analysis, and the peak ground acceleration (P_{GA}) scaled to multiple intensity levels was 0.2g, 0.4g, and 0.6g for design level earthquake (DLE), maximum considered earthquake (MCE), and extremely rare earthquake (ERE), respectively.

Results and Discussions The results illustrated that NVFI significantly reduced the displacement, velocity, and acceleration responses of the SDOF systems subjected to different earthquake records at different hazard levels. The average displacement reduction ratios were 46%, 56%, and 34% for the SDOF–NVFI subjected to far-field, near-fault pulse, and near-fault non-pulse ground motions at the DLE hazard level, respectively. Similar reductions were also observed in the velocity and acceleration results. Compared to the results of the far-field and near-fault non-pulse ground motions, the displacement and velocity responses of the SDOF systems subjected to near-fault pulse ground motions were more effectively decreased using the proposed NVFI while maintaining a basically approximate acceleration mitigation effect. This is attributed to the fact that the proposed NVFI exhibits good energy dissipation capacity, which was induced by its unique friction mechanism. The satisfactory and variable friction force made the NVFI more suitable for buildings under seismic earthquakes with strong uncertainty, especially for near-fault pulse-such as earthquake events. On the other hand, the seismic input energy of the SDOF system was also decreased through the proposed NVFI. The seismic input energy of the SDOF–NVFI system was less than 15 kJ at the MCE hazard level, while the seismic input energy of the SDOF system was greater than 24 kJ. This indicated that the fundamental frequency of the SDOF system can be effectively shifted from the dominant frequency of external disturbance by introducing the proposed NVFI, thus improving the overall performance of the structure. Finally, the parameter analysis of the SDOF–NVFI systems considering different inertance-to-mass ratios was further performed to reveal the influence of the inerter mechanism from the proposed NVFI. The results illustrated that increasing the inertance-to-mass ratio of the proposed NVFI has a significant influence on the velocity and acceleration responses of the SDOF systems at the DLE hazard level while showing a slight but visible influence on the displacement response. Specifically, more than a 10% increase in the velocity and acceleration responses of the SDOF systems subjected to far-field ground motions at the DLE hazard level was observed, with the inertance-to-mass ratio increasing from 0.1 to 0.5.

Conclusions The results indicated that the energy dissipation of the SDOF system primarily depends on the superior energy dissipation capacity of the NVFI due to the effectiveness of its variable friction mechanism, whereas the inerter serves only to transform the seismic input energy.

Key words: non-preload; variable friction; inerter; extremely rare earthquake; seismic performance

（编辑　周　璇）

引用格式: Zhao Guifeng,Liu Wei,Ma Yuhong,et al.Seismic performance analysis of energy dissipation building with non-preload variable friction inerter under extremely rare earthquake[J].Advanced Engineering Sciences,2025,57(4):62–70.[赵桂峰,刘伟,马玉宏,等.极罕遇地震作用下无预紧力变摩擦惯容器消能体系抗震性能分析[J].工程科学与技术,2025,57(4):62–70.]